Extended Abstracts of the 2012 International Conference on Solid State Devices and Materials, Kyoto, 2012, pp68-69

Influence of Structural Parameters on Performance of Schottky Tunneling FET Electrical Characteristics and its Scalability

Yan Wu[1,2,3], C. Dou[1,2,3], K. Kakushima[2], K. Ohmori[4], P. Ahmet[1], T. Watanabe[5], K. Tsutsui[2], A. Nishiyama[2], N. Sugii[2], K. Natori[1], K. Yamada[4], Y. Kataoka[2], T. Hattori[1] and H. Iwai[1]

[1]Frontier Research Center, Tokyo Institute of Technology, [2]Interdisciplinary Graduate School of Science and Engineering, Tokyo Institute of Technology, 4259 Nagatsuta, Midori-ku, Yokohama 226-8502, Japan

[3]Honors Graduate Program for Nanotech/Sciences, University of Tsukuba, [4] Graduate School of Pure and Applied Sciences, University of Tsukuba, 1-1-1 Tennodai, Tsukuba, Ibaraki 305-8573, Japan

[5]Institute for Nanoscience and Nanotechnology, Waseda University Shinjuku, Tokyo 169-8555, Japan

Phone: +81-45-924-5847, Email: yan.w.ab@m.titech.ac.jp

1. Introduction

As the MOSFET scaling goes down to 10nm region, the supply voltage (V_{dd}) and the threshold voltage should be decreased accordingly[1] However, if the threshold voltage is scaled with large subthreshold swing (SS) due to the short channel effect, the current at the zero gate voltage I_{off} would increase. For this reason, devices with sharp subthreshold characteristics have been developed. The tunnel FET is one of the promising candidates to decreases SS. Schottky barrier tunneling FET (SBTFET)[2], which uses Schottky tunnel junction, has many advantages to ordinary PN junction tunnel FETs [3]: low parasitic resistance, better short channel effect (SCE) immunity and high controllability of output characteristics by the silicide material selection. In this work, device simulation has been performed to investigate the structural parameter influence on the electrical characteristics of SBTFETs. With the Schottky barrier height optimization, the SBTFET showed better performance than the conventional SOI-MOS-FET in 10nm region.

2. Simulation and Device Structure.

Silvaco TCAD tool ATLAS (ver.1.3.14.C) with the universal Schottky tunneling model [5] was used for this work. N-type silicon SOIMOS structure (Fig.1) was used in this simulation. Source-to-channel contact is the Schottky contact with various barrier height ϕ_B, while drain-to-channel contact is ohmic (ϕ_B=0). The constant device parameters are the gate oxide thickness (0.3nm), SOI layer thickness (6nm), and BOX thickness (1000nm). The metal gate work function was set to be 4.8eV. The parameters such as ϕ_B, channel carrier concentration (*Na*), tunneling mass (*m**) were varied around default values (ϕ_B=0.61eV, *Na*=2x10^{19}cm^{-3}, *m**=0.08[6]). Through all *Na* value, this device is the fully depleted SOIMOS. The drain voltage is set to be 0.3V.

3. Result and Discussion

Figures 2 and 3 show the I_D-V_G and SS characteristics of SBTFET for various ϕ_B and *Na* for long channel (L_G=50nm). *I*d in SBTFET consists of the thermionic component I_{TH} and the tunneling component I_{TN}. The characteristics only for I_{TH} are also shown in Fig.2, indicating that I_{TH} governs *I*d for low V_G, while I_{TN} dominates high V_G region. It indicated that the SS minima are at the V_G area in which *I*d is governed by I_{TN}. These figures also show that lower ϕ_B and larger *Na* lead to better subthreshold characteristics as a general trend. As an imaginary practice, *m** is modified as shown in Fig.4 and it was confirmed that the lighter tunneling mass would directly leads to sharper subthreshold characteristics as expected. Tunneling rate distribution map at source corner of the devices for ϕ_B:0.81eV (a), and 0.41(b) at V_G =0.45 and 0.55V are shown in Fig.5. For large ϕ_B, the distribution hardly changed with the increase in V_G, while the obvious tunneling probability enhancement was observed for small ϕ_B. This may be due to the drastic enhancement of the tunneling probability for large numbers of electrons near the Fermi level in the source electrode for low ϕ_B. The potential distributions at the source corner for devices (Fig.6) with low *Na* (a) and high *Na* (b) indicate that increase in *Na* leads to the abruptness of the potential, resulting in smaller SS, especially for large V_G area. Comparison between the conventional SOIFET and SBTFET (ϕ_B:0.61eV) indicates that SS of the SBTFET is larger for large L_G but smaller for L_G below 10nm. The SS as a function of L_G is illustrated along with the V_{TH} roll-off in Fig. 8. The SCE of SBTFET is suppressed due to the decrease in the depletion layer width from the source contact as illustrated in Fig.9. I_D-V_G and SS of short channel (L_G=10nm) SBTFET with various *Na* (Fig.10) show large *Na* is desirable for steeper SS as in the case of L_G=50nm. However contrary to the result for long L_G, larger ϕ_B is required for the realization of small SS (Fig.11). Figure 12 shows that the influence tendency of ϕ_B on SS and *I*on/*I*off is totally changed between long and short L_G with the critical length of around 15nm. Considering large *I*on/*I*off in short channel region (~10nm) and the uniformity against L_G fluctuation, we conclude that optimum ϕ_B exists around the mid-value of 0.61eV.

Conclusions

Device simulation of SBTFET revealed that low Schottky barrier and high channel carrier concentration is desirable for steep subthreshold swing due to the larger tunneling probability at source corner of the devices. For the short channel device however larger ϕ_B leads to the suppression of the SCE. As a total, optimum ϕ_B value exists in terms of the large *I*on/*I*off ratio in short channel device and the characteristics uniformity against L_G fluctuation.

Acknowledgements

This work was partially supported by JST-CREST.

References

[1] ITRS roadmap. http://www.itrs.net.
[2] K. Jeon, *et al*, Symp. VLSI Tech., p.121. (2010)
[3] T. Krishnamohan, *et al.*, IEDM2008, p.947.
[4] ATLAS user's manual by Silvaco Inc.
[5]K. Matsuzawa, *et al.*, Trans. Elecron Dev., 47, 103 (2000).
[6] K.-H. Kao, *et al.*, Trans.Electron Dev., 59, 292(2012).

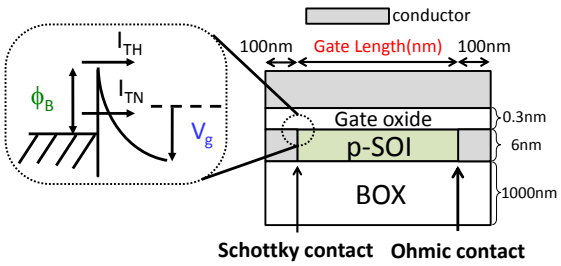

Fig. 1 Device structure and simulation model

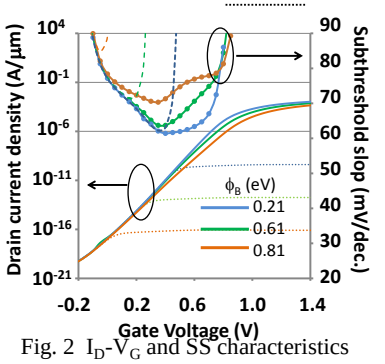

Fig. 2 I_D-V_G and SS characteristics of SBTFET for various ϕ_B (Na=2x10^{19}cm^{-3}) (dot line: only I_{TH} component)

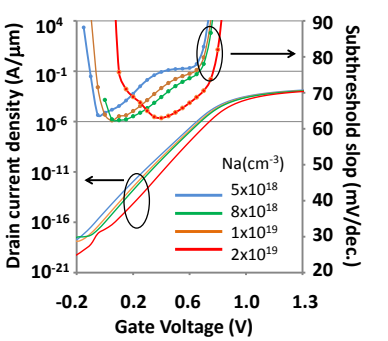

Fig. 3 I_D-V_G and SS characteristics of SBTFET for various Na (ϕ_B =0.61eV)

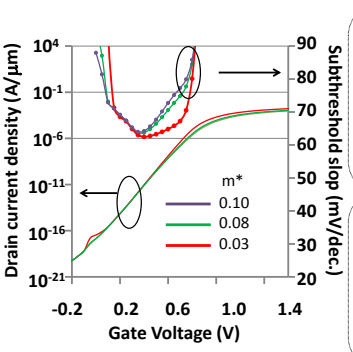

Fig. 4 I_D-V_G and SS characteristics of SBTFET for various m* (Na=2x10^{19}cm^{-3}, ϕ_B =0.61eV)

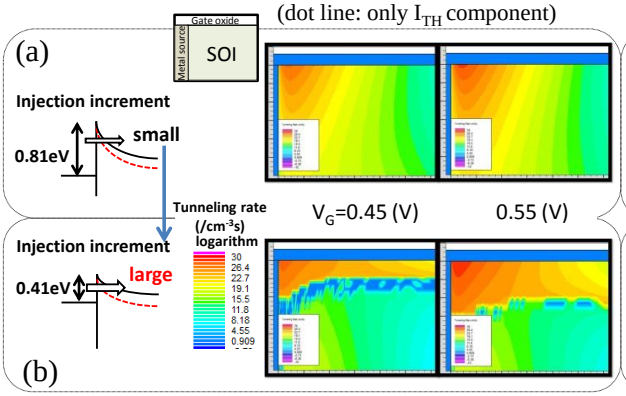

Fig. 5 Band diagram and tunneling rate distribution at subthreshold region. (a) ϕ_B=0.81eV,(b) ϕ_B=0.41eV

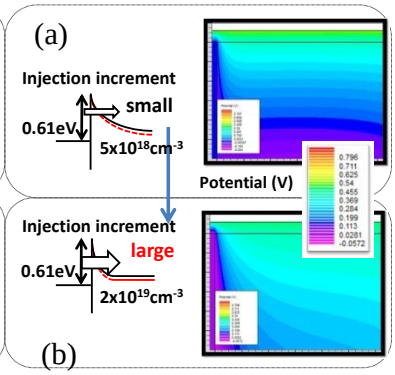

Fig. 6 Band diagram and potential distribution for (a) Na =5x10^{18} (cm^{-3}), (b) Na =2x10^{19} (cm^{-3})

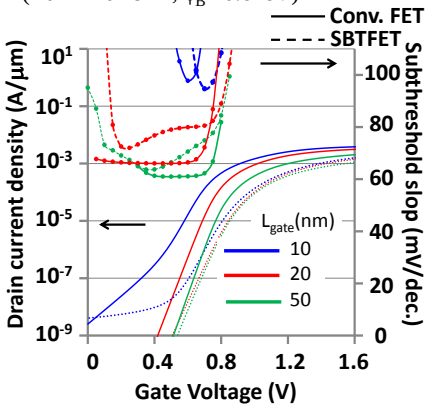

Fig. 7 I_D-V_G and SS characteristics for various L_G. Comparison between conventional FET (solid line) and SBTFET(dot line)

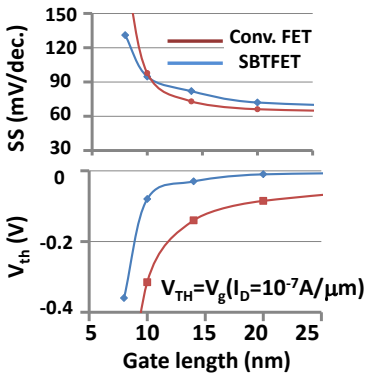

Fig. 8 SS and V_{th} roll-off as a function of L_G. Comparison between conventional FET and SBTFET

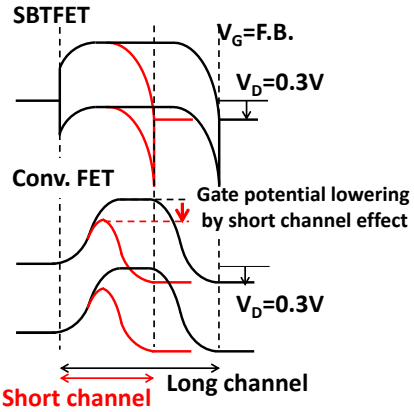

Fig. 9 Band diagram of compare L_G for conventional FET and SBTFET

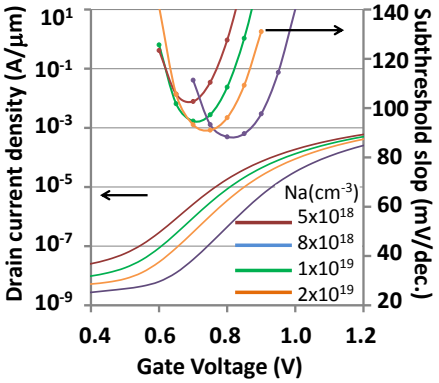

Fig. 10 I_D-V_G and SS characteristics of SBTFET with short L_G for various Na (ϕ_B=0.61eV)

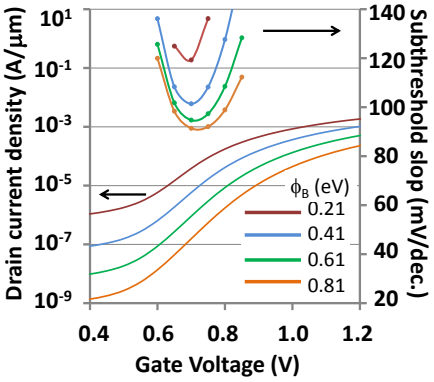

Fig. 11 I_D-V_G and SS characteristics of SBTFET with short L_G for various ϕ_B (Na=2x10^{19}cm^{-3})

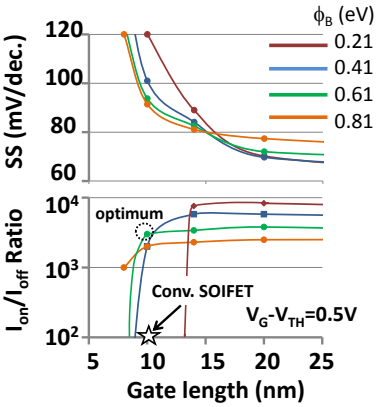

Fig. 12 SS and Ion/Ioff ratio as a function of L_G for various ϕ_B.